

ly there are no measurements for the case with large predicted deviations. Both positive and negative deviations are seen to be possible.

V. CONCLUSIONS

The present results predict that deviations from Blanc's law for both mobility and diffusion coefficients can be of either sign at high fields, and can be of a magnitude that should be detectable experimentally. The deviations depend explicitly on the nature of the ion-neutral interaction through the averages $\langle v_{rj}Q_j \rangle$ and $\langle v_{rj}Q_j \rangle_j$, and are zero for the Maxwell model in which Q_j is inversely proportional to v_{rj} and the mean free time between collisions is

the same at all velocities. This behavior is reminiscent of the behavior of thermal diffusion in neutral gases, which has been used as a sensitive probe of intermolecular forces,¹⁰ and indeed the same sort of averages occur in the momentum-transfer theory of gaseous thermal diffusion.¹¹ This suggests that deviations from Blanc's law at high fields might be a useful probe of ion-neutral forces. Physically, the present theory ascribes the deviations from Blanc's law to the difference in the ion energy partitioning in the gas mixture and in the pure components. Only the particular velocity dependence of the cross section given by the Maxwell model is just right to compensate for this effect.

*Work supported in part by the National Aeronautics and Space Administration under Grant No. NGL-40-002-059.

¹E. W. McDaniel and J. T. Moseley, Phys. Rev. A **3**, 1040 (1971).

²E. A. Mason and H. Hahn, Phys. Rev. A **5**, 438 (1972).

³S. I. Sandler and E. A. Mason, J. Chem. Phys. **48**, 2873 (1968).

⁴R. D. Present, *Kinetic Theory of Gases* (McGraw-Hill, New York, 1958), Secs. 4-2 and 8-3.

⁵G. H. Wannier, Phys. Rev. **87**, 795 (1952).

⁶G. H. Wannier, Bell System Tech. J. **32**, 170 (1953).

⁷J. O. Hirschfelder, C. F. Curtiss, and R. B. Bird, *Molecular Theory of Gases and Liquids* (Wiley, New York, 1964), Chap. 8.

⁸L. D. Higgins and F. J. Smith, Mol. Phys. **14**, 399 (1968).

⁹G. E. Courville and M. A. Biondi, J. Chem. Phys. **37**, 616 (1962).

¹⁰E. A. Mason, R. J. Munn, and F. J. Smith, Advan. At. Mol. Phys. **2**, 33 (1966).

¹¹Reference 4, Sec. 7-1.

Ground State of Two-Dimensional Liquid Helium*

Michael D. Miller and Chia-Wei Woo†

Department of Physics, Northwestern University, Evanston, Illinois 60201
and

Charles E. Campbell

Institute of Theoretical Physics, Department of Physics, Stanford University, Stanford, California 94305

(Received 28 April 1972)

In the interest of understanding the nature and properties of physically adsorbed helium monolayers in the mobile limit, we study the ground state of a two-dimensional helium liquid, using integral-equation techniques which have been thoroughly tested in connection with bulk helium. Our results are compared to those of computer experiments by Hyman and by Campbell and Schick, and to actual experimental data obtained by Dash and co-workers.

As a model for adsorbed helium monolayers, we consider N helium atoms adsorbed on a uniform homogeneous substrate of surface area A . Recent studies¹ of single helium atoms interacting with structured substrates such as graphite indicate that ignoring the structure of the adsorbing surface may be quite realistic for the calculation of some properties of the adsorbate. Specifically, the bands are very broad and overlapping. The resulting high mobility makes it reasonable to expect that the ground-state and low-excited-state properties of interacting helium atoms will not be

significantly modified by the structure of the substrate. The submonolayer heat capacities measured by Bretz and Dash² for He⁴ adsorbed on graphite provide strong experimental evidence for this point of view in the low-density regime. It should be noted, however, that densities which are in registry with adsorption sites provided by the substrate may show a tendency to take advantage of the weak substrate potential at the expense of their mobility, as evidenced by the order-disorder transitions observed in the aforementioned experiments at commensurate densities.³ In that case,

the model under consideration herein does not apply.

With the above discussion in mind, we ignore the structure of the substrate. There remain two roles for it to play. The first one is static: It provides an adsorption potential well in the direction normal to the surface. This well is generally very deep compared to a few degrees Kelvin, and therefore confines the adatoms to motion within the space of the immediate neighborhood of an equilibrium plane at sufficiently low temperatures and densities. The second role of the substrate is dynamic: It mediates the interaction between adatoms, primarily via exchange of substrate excitations like phonons or surfons. According to recent estimates by Schick and Campbell,⁴ these substrate-mediated interactions may be rather insignificant compared to the direct He-He interactions. While a detailed microscopic calculation is necessary⁵ to settle this issue, we will ignore the dynamical role of the substrate and approximate the static role by actually confining all He atoms to their classical equilibrium plane. This results in a two-dimensional many-body problem, that of N He atoms interacting via a pairwise Lennard-Jones potential, moving in a normalization area A , with areal density $n = N/A$ serving alone as a physical parameter.

The excited states of such a model were discussed recently by Jackson.⁶ He adapts Feynman's approach for He⁴ bulk liquid⁷ to the model described above. In order to complete this calculation one requires knowledge of the ground-state wave function which provides correlations for the excited states.

The problem of the ground state was investigated recently by Hyman⁸ using a Monte Carlo method, and by Campbell and Schick⁹ using a molecular-dynamics program developed by Rahman. The results obtained by these authors are consistent insofar as the ground-state energy is concerned, but the equilibrium densities differ by as much as 15%. Their energy-density curves are also incompatible. On account of the small numbers of particles used and the small numbers of configurations (or steps) taken, these computer experiments contain large statistical uncertainties. We report in this note, for comparison, results obtained with several approximate integral equations, whose validity has previously been tested thoroughly in connection with the bulk-helium calculation.¹⁰

The Hamiltonian for the two-dimensional helium system is given by

$$H = -\frac{\hbar^2}{2m} \sum_{i=1}^N \nabla_{\rho_i}^2 + \sum_{1 \leq i < j \leq N} V(\rho_{ij}) \quad (1)$$

where $\vec{\rho}$ has just two components and $V(\rho)$ is taken

to be the Lennard-Jones 6-12 potential with the deBoer-Michels parameters:

$$V(\rho) = 4\epsilon \left[\left(\frac{\sigma}{\rho} \right)^{12} - \left(\frac{\sigma}{\rho} \right)^6 \right] \quad (2)$$

$$\epsilon = 10.22 \text{ }^\circ\text{K}, \quad \sigma = 2.556 \text{ \AA}$$

It should be noted that the method of calculation to be discussed here is not restricted to this potential. If and when the effective He-He interaction under the influence of a dynamical substrate becomes known, we can readily adapt our present program to that more realistic situation. In a way, our work prepares the way for just such a calculation. We believe that the effective interaction will still contain strong repulsion at short distances, not unlike the "hard core" in the Lennard-Jones potential. Our treatment, designed to take into consideration such short-range correlations, will continue to be valid.

The short-range correlations are accounted for at the outset of the calculation through a particular choice of the trial wave function. The shape and range of the short-range correlations are varied to minimize the energy expectation value for every specified areal density. The trial wave function used in our calculations, as well as in Refs. 8 and 9, is of the Jastrow form¹¹:

$$\psi(\vec{\rho}_1, \vec{\rho}_2, \dots, \vec{\rho}_N)$$

$$= \prod_{i < j}^N e^{(1/2)u(\rho_{ij})} / \left(\int \prod_{i < j} e^{u(\rho_{ij})} d\vec{\rho}_1 \dots d\vec{\rho}_N \right)^{1/2} \quad (3)$$

One defines in terms of ψ the l -particle distribution function for the probability density ψ^2 :

$$P^{(l)}(\vec{\rho}_1, \vec{\rho}_2, \dots, \vec{\rho}_l)$$

$$= \frac{N!}{(N-l)!} \int \psi^2(\vec{\rho}_1 \vec{\rho}_2 \dots \vec{\rho}_N) d\vec{\rho}_{l+1} \dots d\vec{\rho}_N \quad (4)$$

The two-particle distribution function

$$P^{(2)}(\vec{\rho}_1, \vec{\rho}_2) = n^2 g(\rho_{12}) = N(N-1) \int \psi^2 d\vec{\rho}_3 \dots d\vec{\rho}_N \quad (5)$$

reduces the energy expectation value to a simple form:

$$\langle H \rangle = \frac{1}{2} N n \int [V(\rho) - (\hbar^2/4m) \nabla_\rho^2 u(\rho)] g(\rho) d\vec{\rho} \quad (6)$$

The variational procedure is then straightforward. One chooses a set of values for the variational parameters placed in $u(\rho)$, and determines $g(\rho)$ in each case. The corresponding pair of $u(\rho)$ and $g(\rho)$ are then substituted into Eq. (6) for evaluating $\langle H \rangle$. At a given areal density, the minimum $\langle H \rangle$ can thus be determined numerically. For a special class of $u(\rho)$, namely, functions which obey simple power laws, a scaling technique is available for calculating the energy minimum as a function of n .

The major task in this program concerns the determination of $g(\rho)$ for a given $u(\rho)$.

In the method of molecular dynamics, $g(\rho)$ is generated by numerically solving the classical equations of motion for N particles, with a distribution of velocities characterized by a temperature T , interacting via a two-body potential $\phi(\rho)$, where

$$\phi(\rho) = -k_B T u(\rho) \quad (7)$$

There are practical limitations on this method. The number of particles considered must not be too large (usually $< 10^3$); this results in finite-size effects. Also, there are limits on the computer time available. Unless the initial conditions are prepared so well as to be near thermal equilibrium, the time required for attaining equilibrium in the system can be painfully long. These limitations frequently lead to large statistical uncertainties. The Monte Carlo procedure suffers from similar restrictions.

Integral-equation methods are available which do not contain statistical uncertainties. They correspond to infinite summations of selected diagrams in the cluster expansion.¹² Clearly the errors involved are determined by the selection process. Over the last ten years or so, a number of detailed calculations have been carried out for bulk helium¹⁰ using integral-equation techniques. We have by now become rather familiar with their properties: both the advantages and the shortcomings. In comparison to computer experiments we find them on the whole more reliable than the short runs like those carried out in Refs. 8 and 9.

First of all, there is the Bogoliubov-Born-Green-Kirkwood-Yvon (BBGKY) equation, which can be readily derived by differentiating Eq. (5) with the gradient operator $\vec{\nabla}_{\rho_1}$:

$$\begin{aligned} \vec{\nabla}_{\rho_1} g(\rho_{12}) &= g(\rho_{12}) \vec{\nabla}_{\rho_1} u(\rho_{12}) \\ &+ (1/n^2) \int P^{(3)}(\vec{\rho}_1, \vec{\rho}_2, \vec{\rho}_3) \vec{\nabla}_{\rho_1} u(\vec{\rho}_{13}) d\vec{\rho}_3. \end{aligned} \quad (8)$$

A hierarchy of equations can be generated if one next differentiates $P^{(3)}$, $P^{(4)}$, etc. For practical applications, one truncates the hierarchy by making the superposition approximation:

$$P^{(3)}(\vec{\rho}_1, \vec{\rho}_2, \vec{\rho}_3) \approx n^3 g(\rho_{12}) g(\rho_{23}) g(\rho_{31}). \quad (9)$$

After some rearrangement, Eq. (8) reduces to

$$\frac{d}{d\rho} \ln g(\rho) = \frac{d}{d\rho} u(\rho) + 2n \int_0^\infty g(\nu) \frac{d}{d\nu} u(\nu) X(\rho, \nu) \nu d\nu, \quad (10)$$

where

$$X(\rho, \nu) = \int_0^\pi g([\rho^2 + \nu^2 - 2\rho\nu \cos\theta]^{1/2}) \cos\theta d\theta. \quad (11)$$

For a given $u(\rho)$, Eqs. (10) and (11) may be solved iteratively. The convergence is rapid if one begins with a good guess for $g(\rho)$. Unexpectedly, however, the solution of the BBGKY equation is far simpler in three dimensions than in two, the reason being that in three dimensions the appearance of the extra factor of $\sin\theta$ greatly expedites the integration over θ .

Next we have the Percus-Yevick (PY) equation

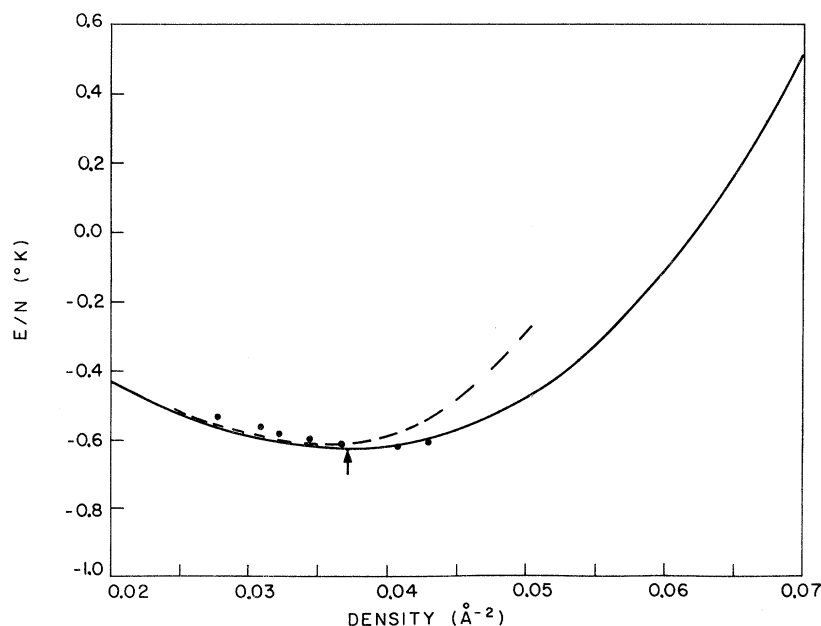


FIG. 1. Total energy per particle obtained from the variational calculation. The solid line is the result of the BBGKY, the dashed line is the molecular-dynamics curve from Ref. 9, and the circles are the Monte Carlo results from Ref. 8. The arrow locates the BBGKY minimum.

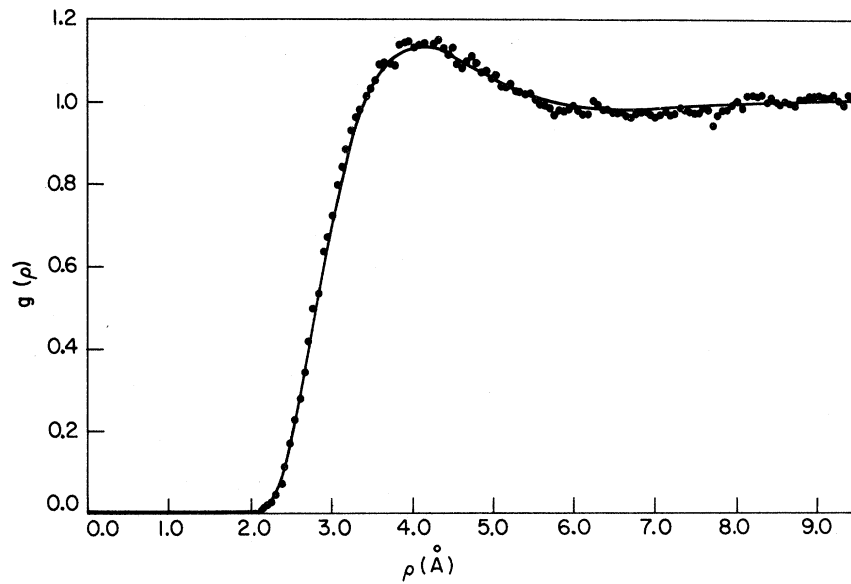


FIG. 2. Radial distribution function at equilibrium density. The solid line is the result of the BBGKY equation and the circles are points from the molecular-dynamics calculation of Ref. 9.

and the hypernetted chain (HNC) equation:

$$\text{PY: } u(\rho) = \ln g(\rho) - \ln [1 + P(\rho)], \quad (12)$$

$$\text{HNC: } u(\rho) = \ln g(\rho) - P(\rho), \quad (13)$$

where

$$P(\rho) = \frac{1}{4\pi^2 n} \int e^{i\vec{k} \cdot \vec{r}} \frac{[S(k) - 1]^2}{S(k)} d\vec{k} \\ = \frac{1}{2\pi n} \int_0^\infty \frac{(S(k) - 1)^2}{S(k)} J_0(k\rho) k dk \quad (14)$$

and

$$S(k) = 1 + n \int e^{i\vec{k} \cdot \vec{r}} [g(\rho) - 1] d\vec{r}$$

$$= 1 + 2\pi n \int_0^\infty [g(\rho) - 1] J_0(k\rho) \rho d\rho. \quad (15)$$

\vec{k} is the two-dimensional momentum vector and $S(k)$ is the two-dimensional liquid-structure function. These equations involve only one-dimensional integrals and are much easier to solve than BBGKY. Also note that if $g(\rho)$ is given instead of $u(\rho)$ these integral equations reduce to mere integrals.

We parametrize $u(\rho)$ in the form

$$u(\rho) = - (a\sigma/\rho)^5, \quad (16)$$

where a is the lone variational parameter.

For BBGKY, the calculations are performed at

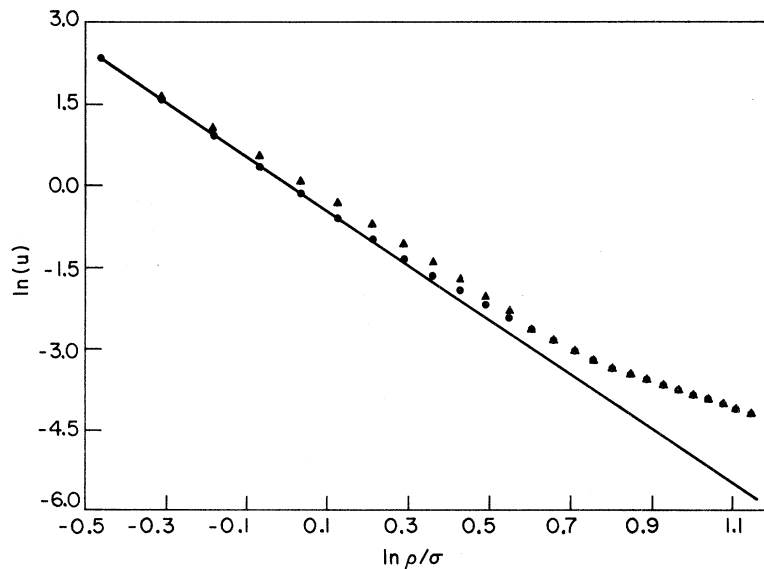


FIG. 3. Comparison of $u(r)$ from a given $g(r)$ using several approximations. The solid line is BBGKY, the circles are PY, and the triangles are HNC.

the density $n_0 = 1/\pi\sigma^2$. It is advantageous to carry out the minimization procedure at a density not too far from the equilibrium density, for then one expects the range of values taken for the variational parameter to be sufficiently wide to surround the energy minimum for all densities of interest. In other words, as we scale our results to other densities, we will not be forced to bring in new values of a in order to pin down the minimum. Since $\pi\sigma^2$ is the only measure of the helium cross-sectional area, we felt that it was a reasonable first approximation for the equilibrium density. Guided by the results of Ref. 9, we take four values of a , solve the BBGKY equation for each case, and evaluate the energy expectation value. Using a scaling technique similar to that described in Ref. 13, we obtain the energy-density relation shown in Fig. 1. The equilibrium density is found to be 0.037 \AA^{-2} , with a ground-state energy of $-0.62 \text{ }^\circ\text{K}$ per atom. Shown in Fig. 2 is the two-particle (radial) distribution function $g(\rho)$ at the equilibrium density. We also show in these figures the results obtained by Hyman⁸ and by Campbell and Schick.⁹ The lateral binding energy is too small to account for the experimental value found by Stewart and Dash¹⁴ for He adsorbed on argon-plated copper. We conclude that in the latter experiment either the substrate exerted mediating effects (static¹⁵ or dynamical⁵), or there were indeed macroscopic surface inhomogeneities. A particular model involving long-range inhomogeneities is shown by Roy and Halsey to account well for this experiment.¹⁶

For PY and HNC, we do not feel that complete variational calculations are necessary. It is much simpler to begin with the $g(\rho)$ determined by BBGKY and compute $u(\rho)$ through Eqs. (12)–(15). Only the kinetic energy

$$\langle K. E. \rangle = \frac{1}{2} N n \int [- (\hbar^2/4m) \nabla_p^2 u(\rho)] g(\rho) d\vec{p} \quad (17)$$

TABLE I. Comparison of kinetic energy per particle for $g(\rho)$ at $n = 0.0487 \text{ \AA}^{-2}$ using several approximations.

a^5	PY ($^\circ\text{K}$)	HNC ($^\circ\text{K}$)	BBGKY ($^\circ\text{K}$)
0.588	3.54	3.69	3.60
1.027	3.91	4.20	4.01
1.958	4.50	5.11	4.66
3.36	5.12	6.43	5.41

will then vary from that obtained with BBGKY. Table I lists the kinetic energy for each value of a at density n_0 . The agreement between PY and BBGKY is generally better than that between HNC and either, much as we expect from our experience with bulk helium. It is interesting to compare the $u(\rho)$ calculated with PY and HNC to the $u(\rho)$ of BBGKY with all three u 's corresponding to the same $g(\rho)$. Such a comparison is shown in Fig. 3 for $a = (1.027)^{1/5}$ at n_0 .

It is true that what we present here is merely a liquid calculation: The wave function employed does not permit crystallization. However, at an areal density of 0.037 \AA^{-2} , the system is about half as dense as bulk liquid helium at equilibrium (zero pressure). It is very unlikely that a solid-like wave function can give rise to a lower energy.⁴

A great deal can be extracted from this work. In particular, when sufficient accuracy is achieved, such a calculation will complete Jackson's earlier work⁶ on the mobile model of the adsorbed helium monolayer. We are in the finishing stages of a highly efficient Monte Carlo calculation, which corroborates the results given here. The details and some interesting findings will be presented shortly elsewhere.

One of us (C-W. W.) wishes to express his gratitude to the University of Washington and Professor J. G. Dash, for the generous hospitality extended him. Part of this work was initiated there.

*Work supported in part by the National Science Foundation through Grant No. GP-29130, by the Advanced Research Projects Agency through the Materials Research Center of Northwestern University, and by the Air Force Office of Scientific Research, Office of Aerospace Research, U. S. Air Force, under AFOSR Contract No. F 44620-71-C-0044.

[†]Alfred P. Sloan Research Fellow.

¹D. E. Hagan, A. D. Novaco, and F. J. Milford, *Proceedings of the Second International Symposium on Adsorption-Desorption Phenomena, Florence, Italy, 1971* (Academic, New York, to be published).

²M. Bretz and J. G. Dash, *Phys. Rev. Letters* **26**, 963 (1971).

³M. Bretz and J. G. Dash, *Phys. Rev. Letters* **27**, 647 (1971).

⁴M. Schick and C. E. Campbell, *Phys. Rev. A* **2**, 1591

(1970).

⁵C-W. Woo, *J. Low Temp. Phys.* **3**, 335 (1970).

⁶H. W. Jackson, *Phys. Rev.* **180**, 184 (1969).

⁷R. P. Feynman, *Phys. Rev.* **91**, 1301 (1953).

⁸D. S. Hyman, Report No. 1273, Material Science Center, Cornell University, 1970 (unpublished).

⁹C. E. Campbell and M. Schick, *Phys. Rev. A* **3**, 691 (1971).

¹⁰P. R. Roach, J. B. Ketterson, and C-W. Woo, *Phys. Rev. A* **2**, 543 (1970), and references quoted therein.

¹¹This same equation is misprinted in Ref. 9, Eq. (3.1), where $i \neq j$ should be replaced by $i < j$.

¹²A. Munster, *Statistical Physics* (Academic, New York, 1969), Vol. 1, p. 636 ff, and references quoted therein.

¹³W. L. McMillan, *Phys. Rev.* **138**, A442 (1965).

¹⁴G. A. Stewart and J. G. Dash, *J. Low Temp. Phys.*

3, 281 (1970); Phys. Rev. A 2, 918 (1970).

¹⁵H-W. Lai, C-W. Woo, and F. Y. Wu, J. Low Temp. Phys. 5, 499 (1971).

¹⁶N. N. Roy and G. D. Halsey, J. Low Temp. Phys.

4, 231 (1971).

PHYSICAL REVIEW A

VOLUME 6, NUMBER 5

NOVEMBER 1972

He³-Limited Drift of Charge Carriers in Superfluid He⁴ ($0.3 < T < 1.0^\circ\text{K}$)*

K. W. Schwarz

*Department of Physics and The James Franck Institute, The University of Chicago,
Chicago, Illinois 60637*

(Received 21 April 1972)

Measurements were made of the mobility of positive and negative charge carriers in He⁴, for He³ impurity concentrations ranging from 10 to 1800 ppm and temperatures in the range $0.3 < T < 1.0^\circ\text{K}$. The excess inverse mobility $e/\mu - e/\mu_0$ was everywhere found to vary linearly with concentration, as expected. For negative carriers, the data are well explained by a hard-sphere scattering model with a collision radius of 21 Å. For positive carriers, the polarization-deficit potential proposed by Bowley and Lekner gives reasonable agreement with experiment, provided a collision radius of 7.0 Å is assumed.

I. INTRODUCTION

If an electric field is applied to a charge carrier in superfluid helium, the carrier rapidly reaches an equilibrium drift velocity such that its rate of momentum loss due to interaction with the elementary excitations of the liquid equals the electric force on the charge. At low fields this drift velocity is proportional to field: $v_D = \mu E$, where the proportionality constant μ is the mobility. Because of the very large effective masses of the charge carriers, μ can be simply related¹ to the cross sections for the scattering of the elementary excitations by the charge-carrier structures. The experimental determination of μ under conditions where rotons, phonons, or He³ impurities are variously dominant has thus proved to be of considerable interest.

He³ scattering can easily be made the dominant momentum-transfer process at low temperatures by adding a small concentration of the impurities to the superfluid. The earliest measurements on He³-limited mobilities were carried out by Meyer and Reif² for $T > 0.5^\circ\text{K}$. More recent work³⁻⁵ has tended to concentrate on the region below 0.3°K , mainly because some particularly novel features are found in this temperature range, but also because at higher temperatures the scattering from phonons and rotons tends to dominate the behavior. Nevertheless, the temperature range above 0.3°K is also of some interest: Recent theoretical attempts^{6,7} to explain the low-temperature results have been at least qualitatively successful, and it is desirable to test these theories over as wide a temperature range as possible.

In the present work we report the measurement

of the He³ contribution to the inverse mobility e/μ in the temperature range $0.3 < T < 1.0^\circ\text{K}$. Because of the high precision of our mobility measurements, the phonon and roton contributions can be subtracted out to yield the He³ term with reasonable accuracy even at quite low concentrations. Comparisons between our results and the predictions of current theories are made in Sec. III.

II. EXPERIMENT

The experimental setup and our techniques of measuring μ have been fully described in a previous paper.⁸ Briefly, a pulse of charge carriers is gated into a drift region of length ~ 30 cm. The pulse crosses this region under the influence of a uniform electric field, and is detected at the other end by a fast electrometer. The time taken to cross the drift space determines the drift velocity. This technique yields μ to an absolute accuracy of better than $\pm 2\%$.

The only new feature of the present experiment was the mechanism for adding known amounts of He³ to the liquid. A calibrated volume was filled with He³ gas, and the pressure measured with a Texas Instruments 145 quartz Bourdon tube gauge. This known quantity of He³ impurities was then released into the lines leading to the experimental chamber. At least 12 h were allowed for the system to come to equilibrium, after which the measured mobilities showed no significant variations with time. The volume (965 cm³) of the experimental chamber was determined simply by filling it with water. Dead-space corrections for the pump lines leading to the experiment were calculated and found to be negligible. The estimated accuracy to which our He³ concentrations were known is